

# The luminosity – spectral index dependence of the X-ray bright Seyfert galaxies

V. A. Sadova, A. V. Tugay\*

Taras Shevchenko National University of Kyiv, Glushkova ave., 4, 03127, Kyiv, Ukraine

X-ray luminosities and spectral indices of 97 bright Seyfert 1 (Sy1) galaxies from the XMM-Newton archive are analysed in this article. Distribution of these values is random, so we conclude that the model of emission should be at least two-parametric. Within the framework of the merging model of active galactic nuclei (AGN), the relation between black hole mass, stage of merging and observable X-ray parameters is proposed.

**Key words:** X-rays: galaxies, galaxies: Seyfert

## INTRODUCTION

The XMM-Newton observation archive is the largest and the most convenient database for the analysis of the X-ray spectra of any celestial bodies including the extragalactic ones. The *Xgal* sample of X-ray galaxies [15, 18] contains more than 4000 XMM sources associated with the galaxies or galaxy clusters. The main goal of compiling *Xgal* was the study of the large-scale structure (LSS) of the Universe in the X-ray band (0.2–15 keV for XMM-Newton). The distribution of the main elements of LSS — filaments, voids and walls — can be recovered for the redshifts up to 0.2 [14, 17]. It was shown in [16, 19] that the most frequent type of X-ray emitting galaxies at such distances is the Seyfert 1 (Sy1). The spectra of the Sy1 galaxies in the Sloan Digital Sky Survey (SDSS) region were analysed in [16]. 30 of them are Compton thin ( $N_H < 10^{25} \text{ cm}^{-2}$ ) and thus their spectra can be correctly fitted with the power law model. The remaining X-ray bright Sy1 galaxies with the radial velocities from 4000 to 39000 km/s are studied in present work. We compiled a list of the most powerful X-ray galaxies in the nearby Universe — the Compton thin Sy1 galaxies. Our goal was to calculate the spectral parameters of these galaxies, to build their distributions and to identify some realistic connection between the observed spectral parameters and the properties of the internal structure of AGNs.

## SAMPLE SELECTION AND X-RAY SPECTRAL ANALYSIS

The statistics of the galaxies considered in this work is the following. There are 582 bright X-ray extragalactic sources outside of the SDSS region. 87 of them are Sy1. The resulting list of bright Sy1 galax-

ies from the *Xgal* sample consists of three parts:

1. 30 Sy1 galaxies in the SDSS region, for which the spectral parameters were obtained previously in [16].

2. 23 galaxies with the spectra built in the present work using the standard XMM SAS package. We get event lists for the PN camera with the `esproc` procedure, filtered them from the solar protons using the parameters  $150 < \text{PI} < 15000$  and `PATTERN=0` and derived the spectra with the `especget` procedure. Background region was selected from the same CCD chip as the source and of the same size.

3. 46 galaxies with the spectra found in the literature. 33 of them were from CAIXA (Catalog of AGNs in the XMM-Newton Archive [3]).

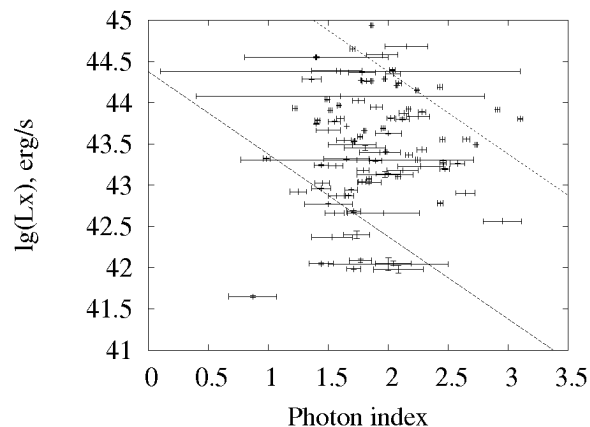


Fig. 1: X-ray parameters of the Sy1 galaxies analysed here. The lower, long-dashed line marks the mass of the central black hole  $M_{\text{BH}} = 10^7 M_{\odot}$ ; for the upper, short-dashed line the black hole mass is  $10^9 M_{\odot}$ .

The parameters of the Sy1 galaxies from p.2 and p.3, except for the CAIXA entries, are presented in

\*tugay.anatoliy@gmail.com

Tables 1 and 2. The main observable parameters of the X-ray emission are the luminosity and the spectral index. In most cases of the Compton thin Sy1 galaxies these are the only parameters that can be fitted correctly. The distribution of these parameters is presented in Fig. 1. Another important spectral feature in the 2–15 keV energy band is the iron emission line at 6.5 keV, but it is rarely detected, so we do not consider it here. Also we find two galaxies where the thermal component dominates the emission: 2E1891 and IRAS05218-1212. We found the best-fit blackbody temperatures of  $1.11 \pm 0.03$  keV and  $2.37 \pm 0.13$  keV for these galaxies respectively. The power law component was not fitted correctly for these galaxies, so they were excluded from further analysis.

## INTERPRETATION OF THE X-RAY LUMINOSITY AND SPECTRAL INDEX

The previously analysed parameters should be connected to some intrinsic parameters of the AGNs. In the model of Hopkins et al. [8] an AGN appears as a result of the collision and merger of two galaxies. Different observable features of that AGN can be interpreted as stages of merging. This model suggests a simple relation of the photon index and the time since the collision:

$$\Gamma = \log(t/10^6 \text{ years}).$$

It was assumed here that at large times after merger the hard X-ray emission decreases that could appear as an increase of the spectral index. Since the central engine of an AGN is assumed to be a supermassive black hole in its centre, the luminosity of that AGN should correlate with the black hole mass. Taking into account the decrease of the luminosity with the age, the following formula for estimating the black hole mass is proposed:

$$\log(M_{\text{BH}}/\mathcal{M}_{\odot}) = \log L_X + \Gamma - A, \quad (1)$$

where  $L_X$  is measured in erg/s. The physical meaning of Eq. (1) lies in the assumption that the total amount of the emitted energy ( $L_X \cdot t$ ) should be related to the total energy budget of the source (or the mass of the available gas, which should be proportional to  $M_{\text{BH}}$ ). This relation, however, has not yet been verified and may have unclear systematical uncertainty behind. The coefficient  $A = 37.375$  was selected to equalise the average black hole mass with the results of a similar work of Vestergaard & Peterson [21] (hereafter VP), where the black hole masses for AGNs were also estimated from the X-ray emission. The averaged logarithm of the black hole mass in [21] and for our sample equals (the uncertainty corresponds to the  $1\sigma$  confidence level):

$$\log(M_{\text{BH}}/\mathcal{M}_{\odot}) = 7.992 \pm 0.562. \quad (2)$$

The two lines corresponding to the black hole mass of  $10^7 \mathcal{M}_{\odot}$  and  $10^9 \mathcal{M}_{\odot}$  are shown in Fig. 1. The derived in this way masses of the central black holes of individual galaxies are presented in the last column of Table 2. The uncertainty of  $\log(M_{\text{BH}}/\mathcal{M}_{\odot})$  depends on the uncertainties of  $\Gamma$ ,  $L_X$  and the systematic effects. According to Eq. (2), this uncertainty should be approximately equal to 0.5 or less. The black hole mass distributions for our sample and VP galaxies were approximated by Gaussian. Deviation for the *Xgal* Sy1 galaxies appears somewhat larger than in [21] —  $\sigma = 0.826$ . This value is potentially biased, as here we study solely the X-ray bright objects, whereas the VP sample, based on the optical data, includes both the X-ray bright and dim sources. The distributions of the black hole masses for our sample and the VP results are presented in Table 3. The percentage of the normal Gaussian distribution is also given for the comparison. The bin width is equal to one standard deviation.

## CONCLUSION AND DISCUSSION

The distribution of the X-ray emission parameters in Fig. 1 is random, so we conclude that the emission model of the studied galaxies should be at least two-parametric. We propose to consider the black hole mass and the merging stage as such intrinsic model parameters. The dependence of the X-ray spectral index on the X-ray luminosity was recently found in [22]. The authors considered the dependence of  $\Gamma$  on  $L_X/L_{\text{Edd}}$  ratio and interpreted this dependence as a two-phase advection dominated accretion. In such study  $L_{\text{Edd}}$  and the black hole mass should be estimated independently from luminosity (for the method of the  $M_{\text{BH}}$  estimation based on the AGN X-ray emission see, e.g. [9]). This is possible if the data on the X-ray variability are available and the same source shows different values of  $\Gamma$  and  $L_X/L_{\text{Edd}}$  in the series of observations. The major part of *Xgal* objects has only one XMM observation available and all the X-ray lightcurves for our Sy1 galaxies are constant. So we can not consider  $\Gamma(L_X/L_{\text{Edd}})$  dependence and conclude here that there is no significant dependence of  $\Gamma$  on  $L_X$ .

## ACKNOWLEDGEMENT

This work was performed at VIRGO.UA. The authors are thankful to the ISDC High-Energy Astrophysics Data Centre for developing the Ukrainian Virtual Roentgen and Gamma Observatory. A. Tugay thanks to anonymous referee for useful comments.

## REFERENCES

- [1] Ballantyne D. R., Fabian A. C. & Iwasawa K. 2004, MNRAS, 354, 839
- [2] Ballantyne D. R. 2005, MNRAS, 362, 1183

- [3] Bianchi S., Bonilla N. F., Guainazzi M., Matt G. & Ponti G. 2009, *A&A*, 501, 915
- [4] Corral A., Barcons X., Carrera F. J., Ceballos M. T. & Mateos S. 2005, *A&A*, 431, 97
- [5] Croston J. H., Hardcastle M. J., Birkinshaw M. & Worrall D. M. 2003, *MNRAS*, 346, 1041
- [6] Gallo L. C., Lehmann I., Pietsch W. et al. 2006, *MNRAS*, 365, 688
- [7] Hardcastle M. J., Sakelliou I. & Worrall D. M. 2005, *MNRAS*, 359, 1007
- [8] Hopkins P. F., Hernquist L., Cox T. J. & Kereš D. 2008, *ApJS*, 175, 356
- [9] Jang I., Gliozzi M., Hughes C. & Titarchuk L. 2014, *MNRAS*, 443, 72
- [10] Lewis K. T., Eracleous M., Gliozzi M., Sambruna R. M. & Mushotzky R. F. 2005, *ApJ*, 622, 816
- [11] Sambruna R. M., Reeves J. N. & Braito V. 2007, *ApJ*, 665, 1030
- [12] Singh V., Shastri P. & Risaliti G. 2011, *A&A*, 532, A84
- [13] Torresi E., Grandi P., Longinotti A. L. et al. 2010, *MNRAS*, 401, L10
- [14] Tugay A. V. 2013, *Advances in Astronomy and Space Physics*, 3, 116
- [15] Tugay A. V. 2012, *Odessa Astronomical Publications*, 25, 142
- [16] Tugay A. V. 2013, *Astronomical School's Report*, 9, 64
- [17] Tugay A. V. 2014, *Advances in Astronomy and Space Physics*, 4, 42
- [18] Tugay A. V. 2014, *IAU Symp.*, 304, 168
- [19] Tugay A. V. & Vasylenko A. A. 2011, *Odessa Astronomical Publications*, 24, 72
- [20] Vasylenko A. A., Zhdanov V. I. & Fedorova E. V. 2015, *Ap&SS*, 360, 37
- [21] Vestergaard M. & Peterson B. M. 2006, *ApJ*, 641, 689
- [22] Yang Q.-X., Xie F.-G., Yuan F. et al. 2015, *MNRAS*, 447, 1692

Table 1: General parameters of the new Seyfert 1 galaxies added to the analysis. The rest of the sample see in [16].  $u$  is the  $u$ -band apparent magnitude;  $r$  is a major semiaxis of the  $25^m$  contour;  $V_{3K}$  is the radial velocity in the CMB reference frame. The parameters were taken from the Hyperlede database.

N	Name	RA, deg	DEC, deg	Coord. num.	$u$	$r$ , arcsec	$V_{3K}$ , km/s
1	2MASX J00044124+0007113	1.1718	0.1198	0004+0007	18.63	6.3	31923
2	ESO 540-1	8.5571	-21.4389	0034-2126	13.71	37.8	7744
3	2MASX J00440466+0101531	11.0195	1.0313	0044+0101	17.77	9.3	33210
4	2MASX J00565517-7513524	14.2297	-75.2312	0056-7513	15.04	6.4	22137
5	Mrk 993	21.3812	32.1360	0125+3208	14.37	47.6	4380
6	3C 59	31.7590	29.5128	0207+2930	17.44	11.1	32612
7	UGC 1841	35.7989	42.9914	0223+4259	13.75	65.7	6167
8	2MASX J02491286-0815254	42.3036	-8.2571	0249-0815	16.64	14.0	8617
9	ESO 359-19	61.2570	-37.1876	0405-3711	15.52	17.3	16476
10	3C 111	64.5885	38.0266	0418+3801	19.75	10.0	15305
11	Mrk 1506	68.2962	5.3542	0433+0521	15.06	23.3	9839
12	ESO 15-11	68.8183	-78.0323	0435-7801	15.58	20.3	18351
13	RBS 560	69.3672	-47.1916	0437-4711	16.61	7.4	15574
14	UGC 3142	70.9449	28.9718	0443+2858	15.84	28.0	6434
15	Pictor A	79.9570	-45.7789	0519-4546	16.25	14.7	10516
16	IRAS 05218-1212	81.0288	-12.1693	0524-1210	15.70	7.6	14721
17	2E 1644	95.7820	-64.6060	0623-6436	17.06	15.0	36197
18	2MASX J07185777+7059209	109.7410	70.9891	0719+7059	17.40	5.9	19810
19	2E 1891	119.5000	39.3414	0754+3928	15.21	2.0	28935
20	Sextans Ring	150.5010	-8.1614	0959-0809	15.22	13.0	4910
21	MCG +11-19-030	239.2650	63.8408	1557+6350	15.42	20.8	9000
22	2MASX J16115141-6037549	242.9640	-60.6319	1611-6037	14.70	26.7	4777
23	2MASX J16174561+0603530	244.4400	6.0649	1617+0603	16.19	14.4	11479
24	Mrk 883	247.4700	24.4439	1629+2426	15.78	18.1	11447
25	2E 4097	278.7640	32.6964	1835+3241	15.15	21.2	17289
26	FRL 339	302.9930	-57.0868	2011-5705	16.12	14.4	16274
27	4C 74.26	310.6560	75.1341	2042+7508	15.33	2.0	31071
28	Mrk 509	311.0410	-10.7235	2044-1043	13.35	17.7	10045
29	2MASX J21022164+1058159	315.5900	10.9711	2102+1058	14.92	12.6	8336
30	2MASX J22191855+1207531	334.8270	12.1315	2219+1207	17.19	8.3	24229
31	3C 445	335.9570	-2.1036	2223-0206	17.26	8.9	16510
32	NGC 7469	345.8150	8.8739	2303+0852	12.90	41.4	4545
33	NGC 7589	349.5650	0.2612	2318+0015	15.23	28.7	8578
34	NGC 7603	349.7360	0.2440	2318+0014	14.04	36.1	8484
35	NGC 7720	354.6230	27.0317	2338+2701	13.43	45.4	8695
36	MCG -05-01-013	359.3665	-30.4613	2357-3027	14.96	16.9	8744

Table 2: X-ray parameters of the studied Sy1 galaxies.  $F_X$  is the X-ray flux in the 2–10 keV band in units of  $10^{-14}$  erg/s/cm $^{-2}$ ;  $L_{X40}$  is the X-ray luminosity in the redshift space, computed for  $H = 70$  km/s/Mpc and divided by  $10^{40}$  erg/s;  $\Gamma$  is the spectral index;  $N_H$  is the neutral hydrogen column density; for the spectra fitted in this work the  $\chi^2$ /d.o.f. value is given instead of the reference.

N	Target	$F_X$	$\Delta F_X$	$L_{X40}$	$\Gamma$	$\Delta\Gamma$	$N_H, 10^{20}\text{cm}^{-2}$	Ref.	$\log(M_{\text{BH}}/\mathfrak{M}_{\odot})$
1	0004+0007	45.6	1.9	1080	1.840	0.098	0.013±0.011	28.46/29	7.873 ±0.233
2	0034-2126	80.1	2.2	112	1.440	0.100		[6]	6.489 ±0.235
3	0044+0101	110.5	8.7	2831	1.806	0.174	0.063±0.027	74.98/34	8.258 ±0.309
4	0056-7513	557.0	14.6	6339	2.118	0.056	0.046±0.008	113.13/61	8.920 ±0.191
5	0125+3208	216.6	3.4	96	1.710	0.060	0.07±0.01	[4]	6.694 ±0.195
6	0207+2930	1434.4	4.5	35428	1.398	0.006	0.0013±0.0007	4765.6/998	8.947 ±0.141
7	0223+4259	50.4	1.4	45	0.870	0.200		[5]	5.518 ±0.335
8	0249-0815	65.3	4.2	113	2.041	0.151	0.013±0.015	18.07/23	7.094 ±0.286
9	0405-3711	612.4	7.9	3861	1.764	0.019	0±0.006	28.12/17	8.351 ±0.154
10	0418+3801	8202.2	17.5	44619	1.700	0.020	0.8	[10]	9.349 ±0.155
11	0433+0521	8159.1	16.0	18343	1.860	0.010	0.01±0.001	[1]	9.122 ±0.145
12	0435-7801	251.9	4.2	1970	1.894	0.050	0.051±0.008	78.48/65	8.188 ±0.185
13	0437-4711	1203.9	5.6	6781	2.247	0.097	0±0.001	598.7/248	9.078 ±0.232
14	0443+2858	2179.5	16.2	2095	0.985	0.029	1.217±0.045	498.34/211	7.307 ±0.164
15	0519-4546	1784.9	4.7	4584	1.800	0.010	0.03±0.01	[20]	8.461 ±0.145
16	0524-1210	454.4	8.6	2287	9.500	9.900	0.909±0.464	143.54/28	-
17	0623-6436	818.0	8.4	24890	2.034	0.025	0.021±0.003	246.18/213	9.430 ±0.160
18	0719+7059	147.5	12.3	1344	1.971	0.235	0.024±0.045	2.15/5	8.098 ±0.490
19	0754+3928	382.1	5.0	7429	7.372	0.621	0.234±0.043	396.04/40	-
20	0959-0809	1078.5	6.7	604	2.432	0.023	0.066±0.002	783.18/540	8.213 ±0.158
21	1557+6350	50.7	6.0	95	2.082	0.206	0±0.072	5.77/5	7.061 ±0.476
22	1611-6037	907.8	27.7	481	1.712	0.059	0.131±0.016	67.21/56	7.394 ±0.194
23	1617+0603	1596.9	14.6	4887	1.957	0.017	0.021±0.002	535.78/495	8.646 ±0.152
24	1629+2426	287.9	4.2	876	1.689	0.054	0.103±0.014	53.73/57	7.632 ±0.189
25	1835+3241	6930.5	24.1	48110	2.150	0.180	3±1	[13]	9.832 ±0.315
26	2011-5705	296.9	3.8	1826	2.576	0.062	0.039±0.006	94.80/67	8.838 ±0.197
27	2042+7508	3857.2	10.0	86479	1.860	0.010	0.183	[2]	9.797 ±0.145
28	2044-1043	8290.5	10.2	19427	1.970	0.010	0.27±0.01	[20]	9.258 ±0.145
29	2102+1058	154.8	17.6	250	1.736	0.108	0.131±0.025	28.12/17	7.134 ±0.376
30	2219+1207	466.2	4.1	6356	3.099	0.019	0.074±0.002	523.61/233	9.902 ±0.154
31	2223-0206	875.2	12.0	5540	1.4	0.1	1 – 10	[11]	8.143 ±0.235
32	2303+0852	5311.5	14.5	2548	1.980	0.010	45±2	[20]	8.387 ±0.145
33	2318+0015	71.2	2.7	122	1.768	0.093	0.036±0.021	11.84/21	6.854 ±0.228
34	2318+0014	4597.2	32.9	7685	2.280	0.030	14.8±5.6	[12]	9.165 ±0.165
35	2338+2701	62.9	12.1	110	2	0.5	0.5±0.2	[7]	7.041 ±0.905
36	2357-3027	1060.8	46.5	1884	2.455	0.028	0.096±0.002	401.5/302	8.729 ±0.163

Table 3: Distribution of the black hole masses. The intervals are measured in standard deviations.

Interval	< -3	(-3, -2)	(-2, -1)	(-1, 0)	(0, 1)	(1, 2)	(2, 3)	> 3
Number of galaxies	1	2	14	28	37	15	0	0
%	1.0	2.1	14.4	28.9	38.1	15.5	0	0
Number of galaxies in [21]	1	0	1	12	13	5	0	0
%	3.1	0	3.1	37.5	40.6	15.6	0	0
Normal distribution. %	0.2	2.1	15.6	32.1	32.1	15.6	2.1	0.2